

Article

Successes and Issues in the Growth of Mo_{ad} and MoSe_2 on $\text{Ag}(111)$ by the E-ALD Method

Martina Vizza ¹, Andrea Giaccherini ^{2,3,*} , Walter Giurlani ¹ , Maurizio Passaponti ¹, Nicola Cioffi ⁴ , Rosaria Anna Picca ⁴ , Antonio De Luca ¹, Lorenzo Fabbri ¹, Alessandro Lavacchi ⁵, Filippo Gambinossi ¹ , Emanuele Piciollo ⁶, Emanuele Salvietti ¹  and Massimo Innocenti ^{1,*} 

¹ Chemistry Department, University of Florence, Via Lastruccia 3-13, I-50019 Sesto Fiorentino (FI), Italy; martina.vizza@stud.unifi.it (M.V.); walter.giurlani@unifi.it (W.G.); maurizio.passaponti@unifi.it (M.P.); antonio.deluca@unifi.it (A.D.L.); lorenzo.fabbri@unifi.it (L.F.); gambinossi@gmail.com (F.G.); emanuele.salvietti@unifi.it (E.S.)

² Earth Sciences Department, University of Florence, Via La Pira 4, I-50121 Firenze, Italy

³ Industrial Engineering Department, University of Florence, Via S. Marta 3, I-50139 Firenze, Italy

⁴ Chemistry Department, University of Bari Aldo Moro, Via E. Orabona 4, I-70125 Bari, Italy; nicola.cioffi@uniba.it (N.C.); rosaria.picca@uniba.it (R.A.P.)

⁵ CNR-ICCOM, Via Madonna del Piano 10, I-50019 Sesto Fiorentino (FI), Italy; alavacchi@iccom.cnr.it

⁶ LEM srl, Via Valiani 55, I-52021 Levane (AR), Italy; emanuele.piciollo@gmail.com

* Correspondence: andrea.giaccherini@unifi.it (A.G.); m.innocenti@unifi.it (M.I.)

Received: 26 November 2018; Accepted: 18 January 2019; Published: 24 January 2019



Abstract: This paper explores the conditions for the electrodeposition of Mo_{ad} (molybdenum adlayer) on $\text{Ag}(111)$ from alkaline aqueous solution. Moreover, the first stages of the growth of MoSe_2 are also presented, performing the deposition of Se_{ad} on the deposited Mo_{ad} . The deposition of Mo_{ad} on $\text{Se}_{\text{ad}}/\text{Ag}(111)$ was also explored. MoSe_2 is of interest due to its peculiar optoelectronic properties, making it suitable for solar energy conversion and nanoelectronics. In this study, electrodeposition techniques were exploited for the synthesis process as more sustainable alternatives to vacuum based techniques. The electrochemical atomic layer deposition (E-ALD) method emerges as a suitable technique to grow inorganic semiconductor thin films thanks to its fulfillment of the green energy predicament and a strict structural and morphological control, and this approach has gathered the attention of the scientific community. Indeed, E-ALD exploits surface limited reactions (SLRs) to alternate the deposition of chemically different atomic layers constituting a compound semiconductor. Thus, E-ALD is one of the most promising electrodeposition techniques for the growth of thin-film of compound semiconductors under a strict structural and morphological control. On this ground, E-ALD can be considered an ideal technique for the growth of 2D materials.

Keywords: E-ALD; MoSe_2 ; 2D materials; nanoelectronics

1. Introduction

One of the main topics in photovoltaic research concerns the study and development of low cost and energy inexpensive processes for the manufacturing of nano and microelectronic devices [1,2]. This subject covers the production of semiconducting material and devices by processes involving the use of reduced amounts of rare elements, consuming less energy and producing less waste. Such technology aims to enable the production of thin films with optimal characteristics for their use in solar cells, limiting the environmental impact. The electrochemical atomic layer deposition (E-ALD) method [3] is one of these techniques, allowing the growth of semiconductor thin films exploiting surface limited reactions (SLRs) [4–7]. One of the most common SLR in electrochemistry is the under

potential deposition (UPD) [7,8]. When the E-ALD outcome is a strictly epitaxial film, the technique is named electrochemical atomic layer epitaxy (ECALE) [9,10]. Indeed, the E-ALD method enables the growth of monolayers of different elements, one above the other through, the alternate deposition of an atomic layer under the surface limited constraints ensured by the exploitation of the SLRs. When the two elements are a chalcogenide and a metal, the process leads to the growth of a binary compound semiconductor. Several successful studies have been reported in this field [11–31]. Most of these papers reported that thin films obtained in this manner could be extremely flat from a morphological standpoint and the crystalline structures are often highly ordered (single crystal and epitaxial deposits). One of the requirements for the occurrence of the whole process is the fast exchange of solution inside the electrochemical cell. To this aim, an apparatus was developed, consisting in an electrochemical cell in which the precursor solutions of the different layers were injected alternatively to obtain the deposition of the various layers under the remote control of an automated system [32,33]. Such a device enabled the growth of an increasingly thicker film. Another requirement for a successful E-ALD study is the correct preparation of a clean electrodic surface. Although not necessary, the use of single crystal electrodes allows a more reliable electrochemical characterization. In this paper, we applied such a method to the growth of MoSe₂ thin films, studying the electrochemical conditions for alternating SLRs in a E-ALD on an Ag(111) electrodic surface. MoS₂ and MoSe₂ are important IV–VI compound semiconductors [34,35], diamagnetic and indirect bandgap semiconductors. Their potential use spans from catalysis to microelectronics, to photonics. Indeed, these compounds fit perfectly with the solar emission, in virtue of their bandgap, which is close to the silicon one and could possibly allow their use as semiconductors in solar cells. Moreover, the bandgap of a few layers of MoSe₂ and MoS₂ can be tuned with the film thickness [36]. They have also peculiar optoelectronic properties, with very deep minima in the band structure, enabling their exploitation for the arising field of valleytronics [37–41]. Nowadays, thin films of MoS₂ and MoSe₂ have been already synthesized with vacuum based techniques [42–44]. The E-ALD process for the growth of MoSe₂ has been already demonstrated on Au(111) by Tsang et al. [45], but not yet on silver; due to the attractive characteristic of the E-ALD, this growth process could revolutionize the production of such interesting material.

2. Materials and Methods

Sigma Aldrich ammonium heptamolybdate tetrahydrate 99% (NH₄)₆Mo₇O₂₄·4H₂O, Merck analytical grade sodium selenite NaSeO₃ and Merck Suprapur[®] (Darmstadt, Germany) NaOH were used without further purification. 12 mL of Merck analytical reagent grade perchloric acid HClO₄ 65% and 10 mL of ammonium hydroxide solution NH₄OH 28% were used to prepare 2 L of the ammonia buffer (pH 9.2).

The water was demineralized and then distilled twice; the second distillation was performed on permanganate while constantly discarding the heads to purify from the volatile organic compounds. The solutions were freshly prepared just before each series of measurements. The electrochemical cell was a cylinder (made of Kelef, height 40 mm, internal diameter 10 mm, and external diameter 50 mm). The working electrode was placed at the bottom of the cylinder and the counter electrode on top, the cell volume was 3.1 mL. The solution inlet and outlet were placed on the sidewalls of the cylinder. The counter electrode (a gold disc) facing the working electrode ensured a high homogeneity of the deposits and better electrochemical performances (low ohmic drop). The reference electrode was an Ag/AgCl (saturated KCl) placed in the outlet tubing. To avoid leakage, both the working and the counter electrode were pressed against Viton[®] O-ring with suitable diameters. The working electrode was a Ag(111) single crystal grown in a graphite crucible and cut according to the Bridgman technique [46,47]. As a first step of the surface conditioning, the electrode was chemically polished with CrO₃ (Hamelin et al. [48]). Then, the electrode surface was cleaned in concentrated sulfuric acid for about 20 min and then rinsed thoroughly with bi-distilled water. As a final step for the treatment, cathodic and anodic conditionings of the surface were performed in the pH 9.2 ammonia buffer. To this aim, a potential of –1.6 V was applied to the working electrode for 1 minute, then, after the injection of

a fresh buffer solution in the cell, a potential of -0.1 V was applied for 1 minute. Both the distribution valve and the cell were designed and realized in the workshop of the Applied Electrochemistry Lab of the University of Florence [10]. The potentials reported in this paper are referred to the Ag/AgCl (saturated KCl) reference electrode.

3. Results

3.1. Deposition of Mo Atomic Layers on Ag(111)

The deposition of Mo from $(\text{NH}_4)_6\text{Mo}_7\text{O}_{24}\cdot 4\text{H}_2\text{O}$ 1 mM was performed in a pH 9.2 ammonia buffer. The predominant species in the working solution (pH 9.2 and a concentration of molybdenum of 7 mM) is the monomeric ion MoO_4^{2-} . The MoO_4^{2-} in aqueous solutions reaches the equilibrium quickly with the polymeric molybdate species $[\text{Mo}_7\text{O}_{24}]^{6-}$. At pH below 6, polymerisation of MoO_4^{2-} occurs through linking of MoO_6 octahedra, yielding the heptamolybdate ion $[\text{Mo}_7\text{O}_{24}]^{6-}$ (pH 5–6) and the octamolybdate ion $[\text{Mo}_8\text{O}_{26}]^{4-}$ (pH 3–5). [49]. Figure 1 shows the voltammograms of the solution 7 mM MoO_4^{2-} in a pH 9.2 ammonia buffer solution on Ag(111). The increase in the cathodic current at -0.26 V (C1) is not yet completely clear and has the shape of a very wide peak. Setting the potential end of the cyclic voltammogram to a more negative value, first a reduction peak appears at -0.8 V, and at -0.9 V, a second reduction process occurs. The peak at -0.8 V (C2) is very close to the bulk reduction potential, which overlaps partially. According to the literature [45], these peaks correspond to MoO_4^{2-} reduction to Mo(0), however, we cannot exclude that during the deposition there was no formation of a MoO_x species.

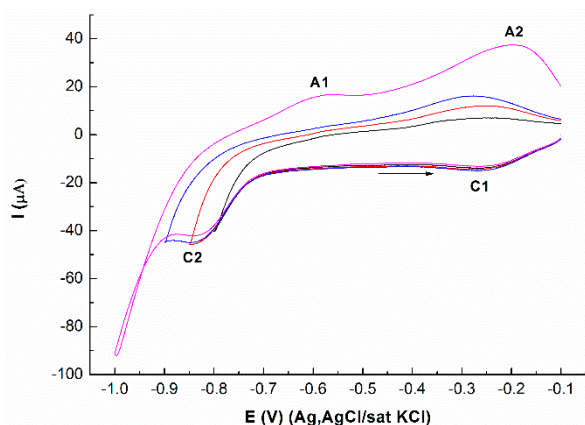


Figure 1. Cyclic voltammograms of 7 mM MoO_4^{2-} on Ag(111) in a pH 9.2 ammonia buffer solution, different end scan. The scan rate is $50 \text{ mV}\cdot\text{s}^{-1}$.

The anodic scan shows two peaks at -0.56 V (A1) and -0.19 V (A2), which are probably related to the oxidation of Mo to MoO_2 , and in a conversion of the insoluble MoO_2 to soluble MoO_4^{2-} , respectively.

Further analysis was performed to understand the reduction processes better.

Figure 2 shows the anodic stripping curves of Mo at different deposition potentials from -0.60 to -0.85 V, at a constant accumulation time of 15 min.

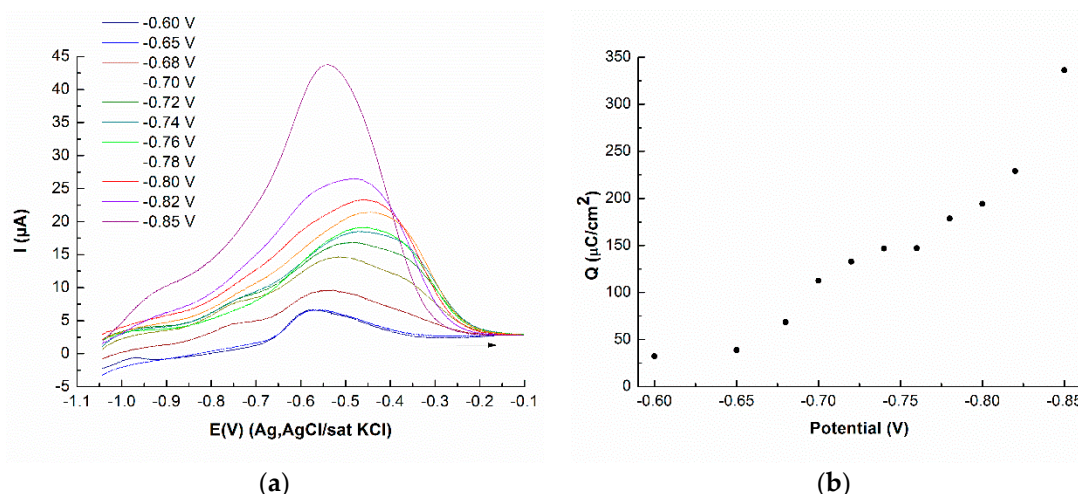


Figure 2. (a) Anodic stripping curves after potentiostatic deposition of Mo at different potentials (deposition time 15 min) on Ag(111) in NaOH 0.1 M. The scan rate is $50 \text{ mV}\cdot\text{s}^{-1}$. (b) Plot of the charge density (Q) involved in the stripping of Mo deposited on Ag(111) as a function of the deposition potential, at a constant deposition time of 15 min.

As elsewhere discussed [7,17,33,50], a way to reveal the surface limited character of an electrodeposition process is to study the charges measured in the previous anodic stripping as a function of the deposition potential and deposition time as shown in Figures 2b and 3b. Figure 2b shows the stripping charges of the deposit obtained at different potential values, while the concentration and deposition time were kept constant. The charge (Q) versus potential curve exhibits a plateau from -0.74 and -0.76 V (Figure 2b). This range corresponds to the optimum potentials for the SLR.

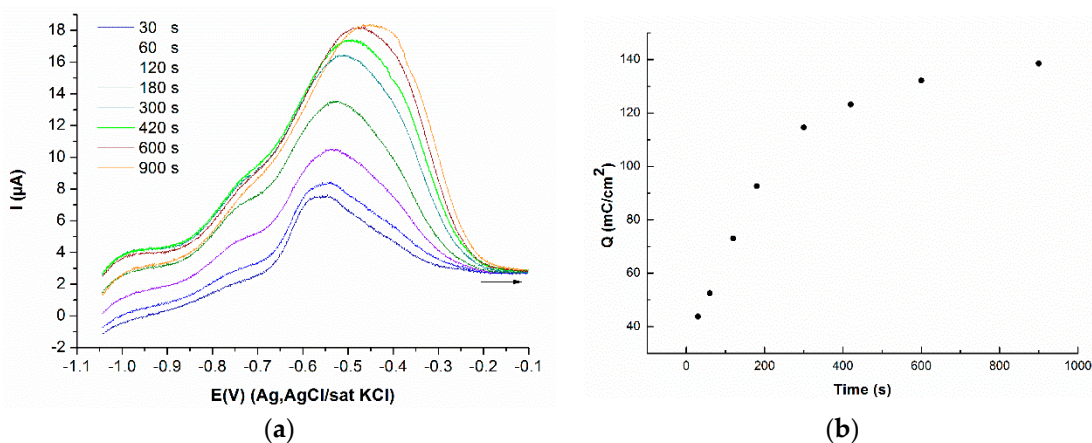


Figure 3. (a) Anodic stripping curves of Mo deposited at $E = -0.75$ V on Ag (111) in NaOH 0.1 M. The scan rate is $50 \text{ mV}\cdot\text{s}^{-1}$. The curves refer to deposition times from 30 s to 15 min (b) Plot of the charges, Q , involved in the stripping of Mo deposited on Ag(111), as a function of the accumulation time, at a constant deposition potential of -0.75 V.

In Figure 3, the charges measured in the previous anodic stripping of the deposited Mo are reported as a function of the accumulation time, at constant concentration and deposition potential (-0.75 V). The asymptotic trend was expected as we have a process limited by the surface. Then, the Mo can be underpotentially deposited on Ag(111), applying a potential at -0.75 V for 15 min. This procedure is very critical because at potentials more negative than -0.76 V, the Mo bulk deposition started.

3.2. Deposition of Se on Atomic Layer of Mo on Ag(111)

The electrochemical characterization presented in the previous paragraph allowed the defining of a suitable set of parameters for the surface limited electrodeposition of an atomic monolayer of Mo on the Ag(111). The Mo ad-layer on Ag(111) ($\text{Mo}_{\text{ad}}/\text{Ag}(111)$) can be deposited by applying a potential of -0.75 V for 15 minutes to the solution of 7 mM MoO_4^{2-} in ammonia buffer pH 9.2. In the following, the deposition of Se on $\text{Mo}_{\text{ad}}/\text{Ag}(111)$ will be explained. Figure 4 reports the voltammograms of 1 mM SeO_3^{2-} in a pH 9.2 ammonia buffer solution on $\text{Mo}_{\text{ad}}/\text{Ag}(111)$.

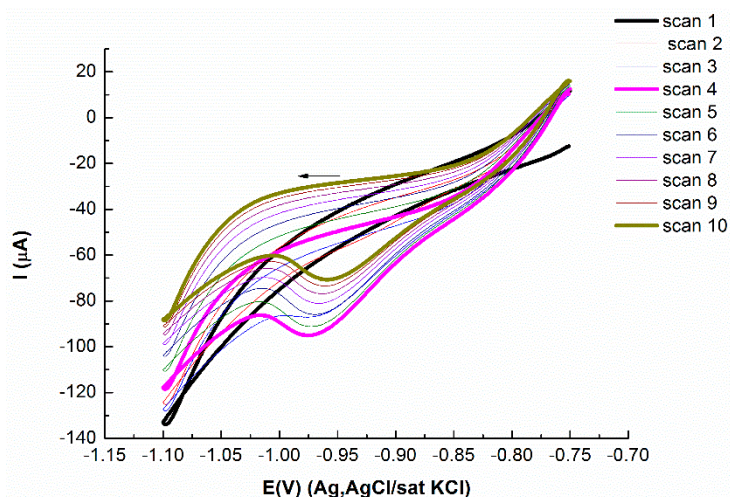


Figure 4. Consecutive cyclic voltammograms of 1 mM SeO_3^{2-} on $\text{Mo}_{\text{ad}}/\text{Ag}(111)$ in a pH 9.2 ammonia buffer solution, different end scan. The scan rate is $50 \text{ mV}\cdot\text{s}^{-1}$.

The voltammograms were registered at a more negative potential than the dissolution of Mo. The charge involved in the cathodic peak at -0.97 V reached a limiting value after five scans. In analogy, with what happens on Ag, this peak can be attributed to the bulk reduction of $\text{Se}(0)$ to $\text{Se}(-\text{II})$ [51]; in our case, in the presence of Mo, this reaction was anticipated at about 30 mV . The positive current at -0.75 V indicates the reoxidation of $\text{Se}(-\text{II})$ to $\text{Se}(0)$. Then, the procedure to obtain a layer of selenium consists in producing $\text{Se}(-\text{II})$ at -1.10 V, keeping constant the potential at -0.85 V for 5 min (to avoid reoxidation of $\text{Se}(-\text{II})$), to form $\text{Se}(0)$ by comproportionation, and finally a washing step with the solution of the supporting electrolyte at -0.85 V for 1 min to reduce bulk selenium. Figure 5 shows cathodic stripping curves of the deposited Se as a function of the accumulation time, at a constant concentration and deposition potential.

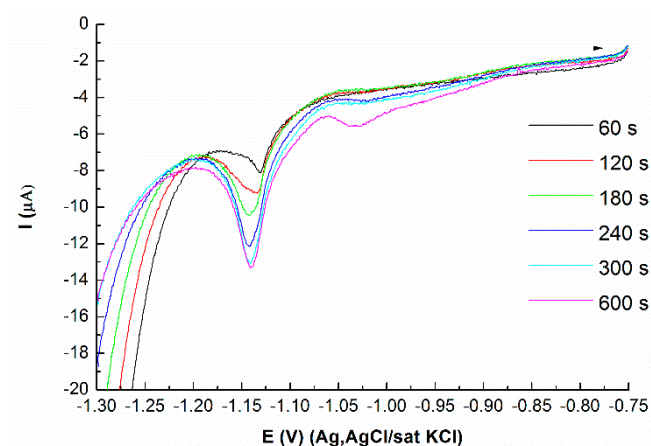


Figure 5. Cathodic stripping curves of Se deposited at $E = -0.85$ V on $\text{Mo}_{\text{ad}}/\text{Ag}(111)$ in $\text{NaOH } 0.1\text{M}$. The scan rate is $10 \text{ mV}\cdot\text{s}^{-1}$. The curves refer to deposition times from 1 to 10 min.

The area of the peak at -1.14 V reached a constant value when performed after 5 min of accumulation time (-0.85 V for 5 min), with the area under the curve being $37.6 \mu\text{C}\cdot\text{cm}^{-2}$.

3.3. Deposition of Mo on Atomic Layer of Se on Ag(111)

To produce a 2D film of MoSe_2 on Ag(111), we started the deposition with a Se ad-layer. The formation of the Se atomic layer on Ag(111) was described by Pezzatini et al. [22]. The Se ad-layer was deposited through a two-step procedure, from 1 mM SeO_3^{2-} in a pH 9.2 ammonia buffer solution on Ag(111), by applying a potential of -0.90 V for 1 min, then 1 min at the same potential with the solution of the supporting electrolyte (washing step).

Figure 6 shows the voltammograms of the ammonia buffer pH 9.2 (black) and 7 mM MoO_4^{2-} in ammonia buffer a pH 9.2 solution on $\text{Se}_{\text{ad}}/\text{Ag}(111)$ (red and blue).

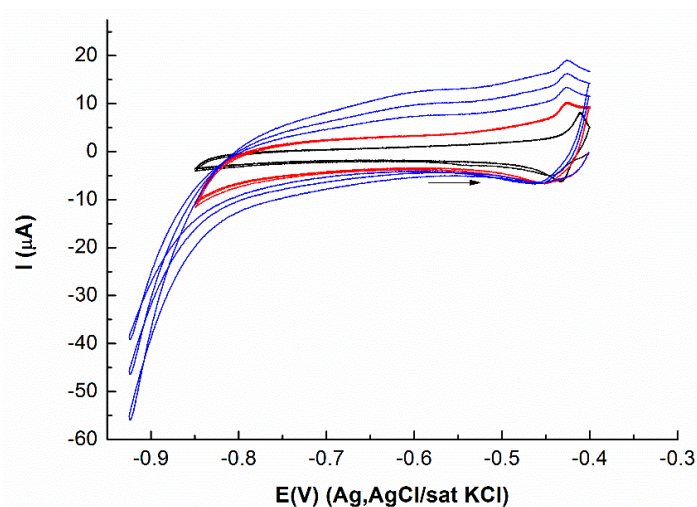


Figure 6. Consecutive cyclic voltammograms of pH 9.2 ammonia buffer solution (black curves) and 7 mM MoO_4^{2-} in a pH 9.2 ammonia buffer solution (red and blue curves, respectively) on $\text{Se}_{\text{ad}}/\text{Ag}(111)$. The scan rate is $50 \text{ mV}\cdot\text{s}^{-1}$.

In the voltammograms of MoO_4^{2-} , in the cathodic scanning, only the beginning of a reduction process is present, and compared to the CV on Ag(111), the peak at -0.8 V is absent. The absence of the peaks before the reduction process at -0.85 V proves that there are no surface limited electrochemical reactions. On this basis, we tried to deposit Mo at the beginning of the reduction process, e.g., at -0.85 V for 1 and 2 min, to verify if this is a bulk deposition (Figure 7).

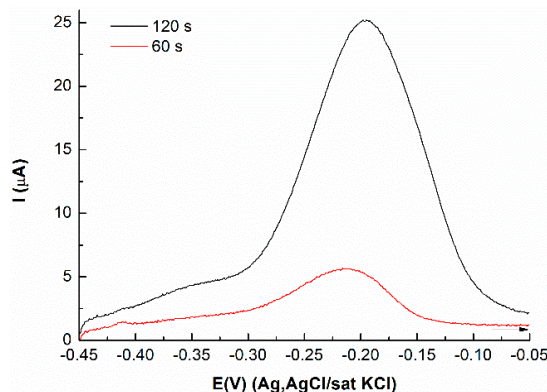


Figure 7. Anodic stripping curves of Mo deposited at $E = -0.85$ V on $\text{Se}_{\text{ad}}/\text{Ag}(111)$ in ammonia buffer pH 9.2 after a -0.45 V washing step. The scan rate is $10 \text{ mV}\cdot\text{s}^{-1}$. The curves refer to deposition times from 1 and 2 min.

The charges measured in the previous anodic stripping of the deposited Mo increased with the deposition time. Furthermore, the charge related to a 2 min-deposition was larger than that of $\text{Mo}_{\text{ad}}/\text{Ag}(111)$. Hence, the MoO_4^{2-} reduction was hypothesized to be a bulk deposition, under the tested conditions.

4. Conclusions

The electrochemical behaviour of MoO_4^{2-} on silver was investigated by cyclic voltammetry and anodic stripping voltammetry, finding results consistent with the study reported by Tsang et al. on $\text{Au}(111)$ [45]. From the analysis of the deposited charges as a function of the accumulation potential and time, we found that Mo_{ad} on $\text{Ag}(111)$ can be deposited by applying a potential of -0.75 V for 15 min to a solution of MoO_4^{2-} . The formation of the Mo_{ad} on $\text{Ag}(111)$ seems a particularly slow process; indeed, the requested accumulation time is high. This may occur because the deposition of Mo on $\text{Ag}(111)$ involves the exchange of seven electrons with the metal substrate. Therefore, this process does not seem to be kinetically favoured. Both the absence of metals other than Mo and the surface limited character of the Mo_{ad} allowed the exclusion of induced codeposition as a mechanism for the growth of the latter [52]. The parameters of electrodeposition of Se on $\text{Mo}_{\text{ad}}/\text{Ag}(111)$ were also investigated, finding the conditions for the growth of the Se ad-layer on $\text{Mo}_{\text{ad}}/\text{Ag}(111)$. The constant peak area of the cathodic stripping voltammetry of Se on $\text{Mo}_{\text{ad}}/\text{Ag}(111)$ after 5 minutes of accumulation time suggests the formation of an ad-layer of Se UPD on $\text{Mo}_{\text{ad}}/\text{Ag}(111)$. However, the deposition of Se on $\text{Mo}_{\text{ad}}/\text{Ag}(111)$ requires a higher accumulation time than the one of Se UPD on $\text{Ag}(111)$, suggesting that the formation of a $\text{Se}_{\text{ad}}/\text{Mo}_{\text{ad}}/\text{Ag}(111)$ is less kinetically favoured than the one of $\text{Se}_{\text{ad}}/\text{Ag}(111)$. In order to produce a 2D film of MoSe_2 on $\text{Ag}(111)$, the electrochemical behaviour of Mo on $\text{Se}_{\text{ad}}/\text{Ag}(111)$ was investigated. The results show that only a bulk deposition of Mo on $\text{Se}_{\text{ad}}/\text{Ag}(111)$ can be obtained in the investigated conditions.

In conclusion, the E-ALD method was used to produce a 2D thin film of $\text{Se}_{\text{ad}}/\text{Mo}_{\text{ad}}/\text{Ag}(111)$, which can potentially be applied in various technological applications, especially in the optoelectronic field [39]. Further investigations are needed to develop the conditions for extending the E-ALD method to the growth of thin MoSe_2 films.

Author Contributions: Conceptualization, A.G. and M.I.; methodology, A.G., A.L. and E.P.; investigation, M.V., E.S., R.A.P., A.D.L. and L.F.; writing—original draft preparation M.V., A.G.; writing—review and editing, A.G., E.S., F.G., W.G., M.P., N.C., R.A.P. and M.I.

Acknowledgments: The authors acknowledge the financial support that has been given from Regione Toscana POR CreO FESR 2014-2020—azione 1.1.5 sub-azione a1 Bando 2 “Progetti di ricerca e sviluppo delle MPMI” which made possible the project “Goielli in Argento Da Galvanica Ecologica e Tecnologica” (GADGET), “Tecnologia al plasma per l’industria del lusso: una manifattura innovativa nel comparto accessori in ottica 4.0” (THIN FASHION).

Conflicts of Interest: The authors declare no conflict of interest.

References

1. Fabricating Energy Devices with Low Environmental Impacts. Available online: <http://www.spie.org/newsroom/6249-fabricating-energy-devices-with-low-environmental-impacts?SSO=1> (accessed on 11 January 2016).
2. Lu, W.; Lieber, C.M. Nanoelectronics from the bottom up. *Nat. Mater.* **2007**, *6*, 841–850. [[CrossRef](#)] [[PubMed](#)]
3. Stickney, B.W.; Gregory, J.L. Electrochemical atomic layer epitaxy (ECALE). *J. Electroanal. Chem.* **1991**, *300*, 543–561.
4. Lay, M.D.; Varazo, K.; Stickney, J.L. Formation of Sulfur Atomic Layers on Gold from Aqueous Solutions of Sulfide and Thiosulfate: Studies Using EC-STM, UHV-EC, and TLEC. *Langmuir* **2003**, *19*, 8416–8427. [[CrossRef](#)]
5. Cavallini, M.; Aloisi, G.; Guidelli, R. In situ STM study of selenium electrodeposition on $\text{Ag}(111)$. *Langmuir* **1999**, *15*, 2993–2995. [[CrossRef](#)]

6. Aloisi, G.D.; Cavallini, M.; Innocenti, M.; Foresti, M.L.; Pezzatini, G.; Guidelli, R. In situ STM and electrochemical investigation of sulfur oxidative underpotential deposition on Ag(111). *J. Phys. Chem. B* **1997**, *101*, 4774–4780. [[CrossRef](#)]
7. Innocenti, M.; Bencista, I.; Di Benedetto, F.; Cinotti, S.; De Luca, A.; Bellandi, S.; Lavacchi, A.; Muniz Miranda, M.; Vizza, F.; Marinelli, F.; et al. Underpotential Deposition of Sn on S-Covered Ag(111). *ECS Trans.* **2013**, *50*, 1–7. [[CrossRef](#)]
8. Oviedo, O.A.; Reinaudi, L.; García, S.G.; Leiva, E.P.M. *Underpotential Deposition: From Fundamentals and Theory to Applications at the Nanoscale*; Springer: Berlin, Germany, 2016; ISBN 9783319243948.
9. Giaccherini, A.; Felici, R.; Innocenti, M. Operando structural characterization of the E-ALD process ultra-thin films growth. In *X-ray Characterization of Nanostructured Energy Materials by Synchrotron Radiation*; IntechOpen: Rijeka, Croatia, 2017.
10. Salvietti, E.; Giaccherini, A.; Gambinossi, F.; Foresti, M.L.; Passaponti, M.; Di Benedetto, F.; Innocenti, M. E-ALD: Tailoring the Optoelectronic Properties of Metal Chalcogenides on Ag Single Crystals. *Semicond. Growth Charact.* **2018**. [[CrossRef](#)]
11. Di Benedetto, F.; Bencistà, I.; Caporali, S.; Cinotti, S.; De Luca, A.; Lavacchi, A.; Vizza, F.; Muniz Miranda, M.; Foresti, M.L.; Innocenti, M. Electrodeposition of ternary $Cu_xSn_yS_z$ thin films for photovoltaic applications. *Prog. Photovolt. Res. Appl.* **2014**, *22*, 97–106. [[CrossRef](#)]
12. Bencistà, I.; Di Benedetto, F.; Innocenti, M.; De Luca, A.; Fornaciai, G.; Lavacchi, A.; Montegrossi, G.; Oberhauser, W.; Pardi, L.A.; Romanelli, M.; et al. Phase composition of Cu_xS thin films: Spectroscopic evidence of covellite formation. *Eur. J. Mineral.* **2012**, *24*, 879–884. [[CrossRef](#)]
13. Lastraioli, E.; Loglio, F.; Cavallini, M.; Simeone, F.C.; Innocenti, M.; Carlaà, F.; Foresti, M.L. In Situ Scanning Tunneling Microscopy Investigation of Sulfur Oxidative Underpotential Deposition on Ag(100) and Ag(110). *Langmuir* **2010**, *26*, 17679–17685. [[CrossRef](#)]
14. Innocenti, M.; Bencistà, I.; Bellandi, S.; Bianchini, C.; Di Benedetto, F.; Lavacchi, A.; Vizza, F.; Foresti, M.L. Electrochemical layer by layer growth and characterization of copper sulfur thin films on Ag(111). *Electrochim. Acta* **2011**, *58*, 599–605. [[CrossRef](#)]
15. Innocenti, M.; Bellandi, S.; Lastraioli, E.; Loglio, F.; Foresti, M.L. Selective electrodesorption based atomic layer deposition (SEBALD): A novel electrochemical route to deposit metal clusters on Ag(111). *Langmuir* **2011**, *27*, 11704–11709. [[CrossRef](#)] [[PubMed](#)]
16. Innocenti, M.; Cattarin, S.; Cavallini, M.; Loglio, F.; Foresti, M.L. Characterisation of thin films of CdS deposited on Ag(111) by ECALE. A morphological and photoelectrochemical investigation. *J. Electroanal. Chem.* **2002**, *532*, 219–225. [[CrossRef](#)]
17. Innocenti, M.; Becucci, L.; Bencistà, I.; Carretti, E.; Cinotti, S.; Dei, L.; Di Benedetto, F.; Lavacchi, A.; Marinelli, F.; Salvietti, E.; et al. Electrochemical growth of Cu-Zn sulfides. *J. Electroanal. Chem.* **2013**, *710*, 17–21. [[CrossRef](#)]
18. Di Benedetto, F.; Cinotti, S.; Guerri, A.; De Luca, A.; Lavacchi, A.; Montegrossi, G.; Carlà, F.; Felici, R.; Innocenti, M. Physical Characterization of Thin Films of $Cu_xZn_yS_z$ For Photovoltaic Applications. *ECS Trans.* **2013**, *58*, 59–65. [[CrossRef](#)]
19. Giaccherini, A.; Russo, F.; Carlà, F.; Guerri, A.; Picca, R.A.; Cioffi, N.; Cinotti, S.; Montegrossi, G.; Passaponti, M.; Di Benedetto, F.; et al. Operando SXRD of E-ALD deposited sulphides ultra-thin films: Crystallite strain and size. *Appl. Surf. Sci.* **2018**, *432*, 53–59. [[CrossRef](#)]
20. Giaccherini, A.; Montegrossi, G.; Di Benedetto, F.; Innocenti, M. Thermochemistry of the E-ALD process for the growth of Cu_xZn_yS on Ag(111): Interpretation of experimental data. *Electrochim. Acta* **2018**, *262*. [[CrossRef](#)]
21. Berretti, E.; Cinotti, S.; Caporali, S.; Cioffi, N.; Giaccherini, A.; Di Benedetto, F.; Foresti, M.L.; Montegrossi, G.; Lavacchi, A.; Vizza, F.; et al. Electrodeposition and Characterization of p and n Sulfide Semiconductors Composite Thin Film. *J. Electrochem. Soc.* **2016**, *163*, D3034–D3039. [[CrossRef](#)]
22. Pezzatini, G.; Caporali, S.; Innocenti, M.; Foresti, M.L. Formation of ZnSe on Ag(111) by electrochemical atomic layer epitaxy. *J. Electroanal. Chem.* **1999**, *475*, 164–170. [[CrossRef](#)]
23. Foresti, M.L.; Milani, S.; Loglio, F.; Innocenti, M.; Pezzatini, G.; Cattarin, S. Ternary CdS_xSe_{1-x} deposited on Ag(111) by ECALE: Synthesis and characterization. *Langmuir* **2005**, *21*, 6900–6907. [[CrossRef](#)] [[PubMed](#)]

24. Gregory, B.W.; Norton, M.L.; Stickney, J.L. Thin-layer electrochemical studies of the underpotential deposition of cadmium and tellurium on polycrystalline Au, Pt and Cu electrodes. *J. Electroanal. Chem.* **1990**, *293*, 85–101. [[CrossRef](#)]
25. Loglio, F.; Innocenti, M.; Jarek, A.; Caporali, S.; Pasquini, I.; Foresti, M.L. Nickel sulfur thin films deposited by ECALE: Electrochemical, XPS and AFM characterization. *J. Electroanal. Chem.* **2010**, *638*, 15–20. [[CrossRef](#)]
26. Russo, F.; Giaccherini, A.; Salvietti, E.; Berretti, E.; Passaponti, M.; Lavacchi, A.; Montegrossi, G.; Piciollo, E.; Di Benedetto, F.; Innocenti, M. Morphology and composition of Cu₂S ultra-thin films deposited by E-ALD. *ECS Trans.* **2017**, *80*, 749–756. [[CrossRef](#)]
27. Innocenti, M.; Cinotti, S.; Bencista, I.; Carretti, E.; Becucci, L.; Di Benedetto, F.; Lavacchi, A.; Foresti, M.L. Electrochemical Growth of Cu-Zn Sulfides of Various Stoichiometries. *ECS Trans.* **2014**, *161*, D14–D17. [[CrossRef](#)]
28. Caporali, S.; Tolstogousov, A.; Teodoro, O.M.N.D.N.D.; Innocenti, M.; Di Benedetto, F.; Cinotti, S.; Picca, R.A.; Sportelli, M.C.; Cioffi, N. Sn-deficiency in the electrodeposited ternary Cu_xSn_yS_z thin films by ECALE. *Sol. Energy Mater. Sol. Cells* **2015**, *138*, 9–16. [[CrossRef](#)]
29. Ceconi, T.; Atrei, A.; Bardi, U.; Forni, F.; Innocenti, M.; Loglio, F.; Foresti, M.L.; Rovida, G. X-ray photoelectron diffraction (XPD) study of the atomic structure of the ultrathin CdS phase deposited on Ag(111) by electrochemical atomic layer epitaxy (ECALE). *J. Electron Spectrosc. Relat. Phenom.* **2001**, *114–116*, 563–568. [[CrossRef](#)]
30. Loglio, F.; Innocenti, M.; D'Acapito, F.; Felici, R.; Pezzatini, G.; Salvietti, E.; Foresti, M.L. Cadmium selenide electrodeposited by ECALE: Electrochemical characterization and preliminary results by EXAFS. *J. Electroanal. Chem.* **2005**, *575*, 161–167. [[CrossRef](#)]
31. Cavallini, M.; Facchini, M.; Albonetti, C.; Biscarini, F.; Innocenti, M.; Loglio, F.; Salvietti, E.; Pezzatini, G.; Foresti, M.L. Two-Dimensional Self-Organization of CdS Ultra Thin Films by Confined Electrochemical Atomic Layer Epitaxy Growth. *J. Phys. Chem. C* **2007**, *111*, 1061–1064. [[CrossRef](#)]
32. Huang, B.M.; Colletti, L.P.; Gregory, B.W.; Anderson, J.L.; Stickney, J.L. Preliminary studies of the use of an automated flow-cell electrodeposition system for the formation of CdTe thin films by electrochemical atomic layer epitaxy. *J. Electrochem. Soc.* **1995**, *142*, 3007–3016. [[CrossRef](#)]
33. Innocenti, M.; Pezzatini, G.; Forni, F.; Foresti, M.L.F. CdS and ZnS Deposition on Ag(111) by Electrochemical Atomic Layer Epitaxy. *J. Electrochem. Soc.* **2001**, *148*, C357–C362. [[CrossRef](#)]
34. Keyshar, K.; Berg, M.; Zhang, X.; Vajtai, R.; Gupta, G.; Chan, C.K.; Beechem, T.E.; Ajayan, P.M.; Mohite, A.D.; Ohta, T. Experimental Determination of the Ionization Energies of MoSe₂, WS₂, and MoS₂ on SiO₂ Using Photoemission Electron Microscopy. *ACS Nano* **2017**, *11*, 8223–8230. [[CrossRef](#)] [[PubMed](#)]
35. Wang, Y.; Zhang, F.; Wang, Q.; Yang, P.; Lin, H.; Qu, F. Hierarchical MoSe₂ nanoflowers as novel nanocarriers for NIR-light-mediated synergistic photo-thermal/dynamic and chemo-therapy. *Nanoscale* **2018**, *10*, 14534–14545. [[CrossRef](#)] [[PubMed](#)]
36. Wilcoxon, J.P.; Samara, G.A. Strong quantum-size effects in a layered semiconductor: MoS₂ nanoclusters. *Phys. Rev. B* **1995**, *51*, 7299–7302. [[CrossRef](#)]
37. Yuan, R.-Y.; Yang, Q.-J.; Guo, Y. Enhanced spin polarization and valley polarization in monolayer MoS₂ junctions. *J. Phys. Condens. Matter* **2018**, *30*. [[CrossRef](#)] [[PubMed](#)]
38. Lu, H.-Z.; Yao, W.; Xiao, D.; Shen, S.-Q. Intervalley Scattering and Localization Behaviors of Spin-Valley Coupled Dirac Fermions. *Phys. Rev. Lett.* **2013**, *110*, 016806. [[CrossRef](#)] [[PubMed](#)]
39. Schaibley, J.R.; Yu, H.; Clark, G.; Rivera, P.; Ross, J.S.; Seyler, K.L.; Yao, W.; Xu, X. Valleytronics in 2D materials. *Nat. Rev. Mater.* **2016**, *1*, 16055. [[CrossRef](#)]
40. Mueed, M.A.; Hossain, M.S.; Jo, I.; Pfeiffer, L.N.; West, K.W.; Baldwin, K.W.; Shayegan, M. Realization of a Valley Superlattice. *Phys. Rev. Lett.* **2018**, *121*, 036802. [[CrossRef](#)]
41. Mak, K.F.; Xiao, D.; Shan, J. Light-valley interactions in 2D semiconductors. *Nat. Photonics* **2018**, *12*, 451–460. [[CrossRef](#)]
42. Wang, X.; Gong, Y.; Shi, G.; Chow, W.L.; Keyshar, K.; Ye, G.; Vajtai, R.; Lou, J.; Liu, Z.; Ringe, E.; et al. Chemical Vapor Deposition Growth of Crystalline Monolayer MoSe₂. *ACS Nano* **2014**, *8*, 5125–5131. [[CrossRef](#)]
43. Boscher, N.D.; Carmalt, C.J.; Palgrave, R.G.; Gil-Tomas, J.J.; Parkin, I.P. Atmospheric Pressure CVD of Molybdenum Diselenide Films on Glass. *Chem. Vap. Depos.* **2006**, *12*, 692–698. [[CrossRef](#)]

44. Chang, Y.-H.; Zhang, W.; Zhu, Y.; Han, Y.; Pu, J.; Chang, J.-K.; Hsu, W.-T.; Huang, J.-K.; Hsu, C.-L.; Chiu, M.-H.; et al. Monolayer MoSe₂ Grown by Chemical Vapor Deposition for Fast Photodetection. *ACS Nano* **2014**, *8*, 8582–8590. [[CrossRef](#)] [[PubMed](#)]
45. Tsang, C.F.; Ledina, M.A.; Stickney, J.L. Molybdenum diselenide formation using electrochemical atomic layer deposition (E-ALD). *J. Electroanal. Chem.* **2017**, *793*, 242–249. [[CrossRef](#)]
46. Hamelin, A. *Modern Aspects of Electrochemistry*; Conway, B.E., White, R.E., Bockris, J.O., Eds.; Plenum Press: New York, NY, USA, 1985; Volume 16, pp. 1–101.
47. Foresti, M.L.; Capolupo, F.; Innocenti, M.; Loglio, F. Visual Detection of Crystallographic Orientations of Face-Centered Cubic Single Crystals. *Cryst. Growth Des.* **2002**, *2*, 73–77. [[CrossRef](#)]
48. Hamelin, A.; Stoicoviciu, L.; Doubova, L.; Trasatti, S. Influence of the crystallographic orientation of the surface on the potential of zero charge of silver electrodes. *Surf. Sci.* **1988**, *201*, L498–L506. [[CrossRef](#)]
49. Aveston, J.; Anacker, E.W.; Johnson, J.S. Hydrolysis of Molybdenum (VI). Ultracentrifugation, Acidity Measurements, and Raman Spectra of Polymolybdates. *Inorg. Chem.* **1964**, *3*, 735–746. [[CrossRef](#)]
50. Foresti, M.; Pezzatini, G.; Cavallini, M.; Aloisi, G.; Innocenti, M.; Guidelli, R. Electrochemical atomic layer epitaxy deposition of CdS on Ag (111): An electrochemical and STM investigation. *J. Phys. Chem. B* **1998**, *102*, 7413–7420. [[CrossRef](#)]
51. Pezzatini, G.; Loglio, F.; Innocenti, M.; Foresti, M.L. Selenium (IV) Electrochemistry on Silver: A Combined Electrochemical Quartz-Crystal Microbalance and Cyclic Voltammetric Investigation. *Collect. Czechoslov. Chem. Commun.* **2003**, *68*, 1579–1595. [[CrossRef](#)]
52. Morley, T.J.; Penner, L.; Schaffer, P.; Ruth, T.J.; Bénard, F.; Asselin, E. The deposition of smooth metallic molybdenum from aqueous electrolytes containing molybdate ions. *Electrochem. Commun.* **2012**, *15*, 78–80. [[CrossRef](#)]



© 2019 by the authors. Licensee MDPI, Basel, Switzerland. This article is an open access article distributed under the terms and conditions of the Creative Commons Attribution (CC BY) license (<http://creativecommons.org/licenses/by/4.0/>).